

Cherenkov Imaged Bio-morphological Features Verify Patient Positioning with Deformable Tissue Translocation in Breast Radiotherapy

Yao Chen, Savannah M. Decker, Petr Bruza, David J. Gladstone, Lesley A. Jarvis, Brian W. Pogue, Kimberley S. Samkoe, Rongxiao Zhang

Abstract (within 300 words)

Significance: Accurate patient positioning is crucial for precise radiotherapy dose delivery, as errors in positioning can profoundly influence treatment outcomes. This study introduces a novel application for loco-regional tissue deformation tracking via Cherenkov image analysis, during fractionated breast cancer radiotherapy.

Aim: The primary objective of this research was to develop and test an algorithmic method for Cherenkov-based regional position accuracy quantification, particularly for loco-regional deformations which do not have an ideal method for quantification during radiotherapy.

Approach: Detection and segmentation of blood vessels was developed in the Cherenkov images using a tissue phantom with incremental movements, and then used in images from fractionated whole breast radiotherapy human imaging (n=10 patients). A rigid and non-rigid combined registration technique was employed to pinpoint inter- and intra-fractional positioning variations.

Results: The developed methodology provides quantified positioning variations, comprising two components: a global shift determined through rigid registration and a two-dimensional variation map illustrating loco-regional tissue deformation, quantified via non-rigid registration. The methodology was tested on an anthropomorphic chest phantom experiment via shifting treatment

couch with known distances and inducing respiratory motion to simulate inter-fraction setup uncertainties and intra-fraction motion respectively, which yielded an average accuracy of 0.83 mm for couch translations up to 20 mm in various directions. Analysis of clinical Cherenkov imaging data from ten breast cancer patients revealed an inter-fraction setup variation of 3.7 ± 2.4 mm compared to the first imaged fraction in the global shift and loco-regional deformations (95th percentile of the vector magnitude) up to 3.3 ± 1.9 mm.

Conclusions: This study introduces the use of Cherenkov visualized bio-morphological features to quantify the global and local variations in patient positioning based on rigid and non-rigid registrations. This new approach demonstrates the feasibility to provide quantitative guidance for inter- and intra-fraction positioning, particularly for the loco-regional deformations that have been unappreciated in conventional in current practice with conventional imaging techniques.

1 Introduction

Breast cancer is the most common malignancy in women, with over 300,000 new cases estimated in 2023.¹ Radiation therapy (RT) has been established as the standard of care for early-stage breast cancer, alone or combined with surgery and chemotherapy, significantly improving local control and survival outcomes.² During RT, the precision of patient positioning is crucial to accurately target the tumor while sparing surrounding healthy tissue.³ Excessive deviations in patient setup or treatment delivery can lead to negative consequences including suboptimal treatment to the tumor, elevated healthy tissue toxicity and secondary radiation induced cancer risks.⁴

With technological advances, X-ray based routine image-guidance including 2D X-ray imaging, 3D cone-beam CT, spontaneous X-ray fluoroscopy and Megavoltage (MV) X-ray portal imaging have been deployed in the standard of care for patient alignment. Optical surface guided radiotherapy (SGRT) has been introduced and developed over the past two decades and is now widely adopted for patient setup verification and monitoring.⁵ Adding to conventional SGRT techniques, Cherenkov imaging has emerged as a non-contact technique for real-time visualization of RT, as depicted in Figure 1A.⁶ Cherenkov light emission occurs when high-energy photon or electron beams interact with tissue, inducing light emission that resembles the radiation beam shape and superficial dose on the patient surface, as shown in Figure 1B.^{7,8} The current implementation of this technique utilizes intensified cameras that are time-gated to synchronize with the linear accelerator pulses, enabling the real-time capture of low-intensity Cherenkov light while effectively suppressing ambient room light.^{9,10} This technology has paved the way for novel applications in RT, including recent studies on inter- and intra-fractional verification of the treatment delivery and error detection.^{9,11}

The passive nature of Cherenkov imaging throughout the entire RT course means that this technique can be used to assess patient positioning accuracy and inform adjustments when needed.⁵ Prior research has showed the efficacy of Cherenkov imaging in detecting incidents that were not identified by other pre-treatment checks, highlighting its unique capabilities.⁹ Further investigations have sought to quantify positioning variations using metrics such as the Dice similarity coefficient and mean distance to conformity (MDC) on binarized images, as well as mutual information (MI) and the γ passing rate (%GP) on non-binarized images, to better detect errors and quantify the magnitude in patient positioning.^{11,12}

Current technologies, including Cherenkov imaging, focus on verifying the global alignment based on rigid image registration.¹³ It is well known that soft tissue deformations exist in the treatment region although quantification of this remains challenging. While reviewing the Cherenkov images acquired from breast RT patients, it was noted that bio-morphological features such as the vasculature were enhanced due to larger optical absorption^{14,15}, which can be observed in Figure 1B. These bio-morphological features could be used as an intrinsic surrogate to quantify the loco-regional deformation. The advantages of using Cherenkov imaged bio-morphological features to quantify the positioning variations are illustrated in Figure 1C – the differences in the bio-morphological features between two fractions, which could be clearly observed visually, reflect the existing setup variations which would be ignored in entire Cherenkov beam regions. More and subtle setup variations have been observed based on the analysis utilizing bio-morphological features compared to utilizing the entire Cherenkov image. Larger setup variations were found between the corresponding bio-morphological features of two fractions compared to their entire Cherenkov beam regions in Figure 1D. These findings inspire the utilization of Cherenkov imaged bio-morphological features to quantify variations in patient positions, particularly from loco-regional deformations that have been neglected or underestimated based on global image analysis.

In this study, we explored utilizing segmented bio-morphological features of the vasculature as internal biological markers in Cherenkov imaging to verify patient positioning accuracy and to inform future image guidance. We employed both rigid and non-rigid registration techniques on Cherenkov images acquired across different fractions (inter-fraction) or within a single fraction

(intra-fraction) to assess positioning accuracy, including the loco-regional deformations that have been neglected to date.

2 Materials and Methods

2.1 Clinical patient imaging

All patient images used in this study were previously collected as part of an Institutional Review Board (IRB)-approved retrospective study at Dartmouth Cancer Center (Lebanon, NH, USA). During their clinically prescribed radiotherapy treatments. Ceiling-mounted cameras continuously monitored for Cherenkov emission and acquired images during all beam-on times, displaying the images in real-time in the control room using BeamSite™ software (DoseOptics LLC, Lebanon, NH, USA). For each treatment fraction, all Cherenkov video frames were summed into a cumulative image representing the total treatment. The Cherenkov video stack and the resulting cumulative Cherenkov image were saved for review. For this study, a total of 10 whole-breast radiotherapy patient Cherenkov data were analyzed.

2.2 Cherenkov image acquisition and processing

Cherenkov light emission during beam delivery was captured by two Cherenkov imaging cameras (BeamSite™, Dose-Optics LLC, Lebanon, NH, USA) fixed to the ceiling of the treatment room. The cameras were angled toward the left and right sides of the treatment couch. These cameras were time-gated for synchronization to the 4 microseconds linear accelerator (LINAC) pulses, allowing rejection of the room light signal in between each pulse. In order to increase the signal-to-background ratio, the system subtracted background images from the raw Cherenkov images, where the background images were acquired immediately after each in-sync

acquisition, followed by spatial and median filtering, as well as dark-field corrections. Details on the routine imaging settings and on-board processing have been described in previous publications.¹⁶

2.3 Quantification methodology

A registration-based methodology utilizing Cherenkov imaged bio-morphological features was developed in this study to quantify patient positioning variations. A flowchart is described in Figure 2A, and each step is illustrated in Figure 2B using a patient example. Image processing was completed in MATLAB version R2023b (MathWorks, Natick, Massachusetts).

2.3.1 Bio-morphological features segmentation

The first step of the quantification methodology is to segment the blood vessels. Due to large optical attenuation by blood in the wavelength of Cherenkov light¹⁷, clear contrast was observed between the vasculature and its surrounding tissues, which make the superficial blood vessel a good candidate to be used as bio-morphological features. A contrast-enhanced filter was applied to the Cherenkov images and manual adjustment of the contrast was employed to assist in the segmentation process. Multiplying the segmented binary vessel region of interest (ROI) mask with the raw cumulative Cherenkov image, a bio-morphological feature image was generated for later image registration step.

2.3.2 Image registration

Image registration was applied to align the segmented bio-morphological features. A rigid and non-rigid combined registration scheme was deployed as shown in Figure 2C. A rigid

registration was performed first to account for global shifts, following by a non-rigid registration to account for the loco-regional deformation.

Rigid registration was performed by using the *imregister* function in MATLAB aiming to minimizing the mean squared error between the bio-morphological features of two fractions, using a regular step gradient descent optimizer technique to solve the rigid image registration through translation and rotation.

Non-rigid registration was performed using a pixel-based B-spline grid based registration algorithm.¹⁸ The algorithm constructed a grid of basis spline control points that control the transformation of the input image and used the squared pixel distance as the similarity measure to evaluate the registration error between moving and static fraction. A quasi-Newton method, limited-memory Broyden-Fletcher-Goldfarb-Shanno (L-BFGS) algorithm,¹⁹ was used as the fast optimizer to move the control points iteratively to achieve the optimal registration between two fractions with minimal registration error.

With the combined scheme of rigid and non-rigid registration, both global shift and local deformation could be quantified from the two types of registration methods respectively. In detail, a global translation indicating the shift in x and y direction was extracted from the transformation matrix of the rigid registration result. A two-dimensional (2D) map with the same size of Cherenkov image indicating the pixel-level local tissue deformation was generated from the iterative process of non-rigid registration result. The magnitude of quantified variations from the registration-based methodology was in units of pixels but then converted to physical

dimension with the unit of millimeter (mm) according to 0.42 mm per pixel conversion factor from the Cherenkov acquisition system.

2.4 Phantom study

Two phantom tasks were designed to test the accuracy of quantifying the inter-fraction and intra-fraction variations respectively. The steps were illustrated in Figure 3A-3D and Figure 3E-3G respectively.

2.4.1 Inter-fraction setup uncertainties

An anthropomorphic chest phantom, displayed in Figure 3A, mimicking the absorption and optical properties of soft human tissue was irradiated with a TrueBeam LINAC (Varian Medical Systems, Palo Alto, CA) with 6 MV X-rays, following an isocentric, left-breast treatment plan designed in Eclipse (Varian Medical Systems, Palo Alto, CA). The plan consisted of two opposing tangent beams from the right anterior oblique (310°) and the left posterior oblique (135°) sides, delivering 266 cGy per fraction. A 2D pattern resembling patient blood vessels was cut from a sheet of neutral density filter and laid flush onto the breast treatment region of the phantom.

The inter-fraction setup uncertainties were simulated by the couch movement. The phantom was initially set up according to the treatment plan and irradiated to obtain a ground truth Cherenkov image illustrated in Figure 3B. To analyze the response of each image similarity metric to patient motion, the treatment couch was systematically shifted laterally, vertically, and longitudinally in steps of 5, 10, and 20 mm from the treatment plan position. At each step, the entire treatment was

delivered, and the cumulative Cherenkov image was recorded, for a total of 9 images for comparison with the image from the static fraction.

The quantification methodology was then performed between the 9 Cherenkov images with varying couch movement and Cherenkov image of the reference fraction as shown in Figure 3C. Rigid registration was performed in order to quantify the linear couch shift. The Cherenkov camera captures variations in the x and y axes of its 2D imaging plane. To translate these observations into clinically relevant movements within the patient's three-dimensional (3D) coordinate system, a trigonometric transformation was applied. This transformation considered the geometric orientation of the camera relative to the couch in the patient coordinate system. The quantified variations in the x and y directions of the Cherenkov imaging plane were projected into the couch's lateral, vertical, and longitudinal shifts based on the angular relationship of the camera's imaging plane to the standard patient coordinate system used in radiation therapy. The quantified couch movement in three directions were then compared to the actual couch movement for testing the accuracy of the methodology and its ability to determine inter-fraction setup errors. Zero mm of discrepancy between quantified and actual couch movement was considered the maximal accuracy of the methodology that should ideally reach.

2.4.2 Intra-fraction motions

The same chest phantom with artificial blood vessels was setup for the quantification of intra-fraction motions illustrated in Figure 3E. The same plan in section 2.4.1 was deployed for the irradiation. The intra-fraction respiratory motion was introduced by a Magellan pneumatically powered ventilator (Oceanic Medical Products, Inc, Atchison, KS, USA) which connected an

oxygen source valve to a cardiopulmonary resuscitation (CPR) manikin lung bag inside the chest phantom through a plastic tube. During this single-fraction treatment, 20 breaths per minute with a tidal volume of 0.75 liter was set for the simulated respiratory motion. Cherenkov video of the entire treatment was recorded with a frame rate of 19.6 frames per second. In order to improve the image signal-to-noise ratio for later quantification methodology, each 20 consecutive frames were summed into a sub-cumulative Cherenkov image. The Cherenkov video of the intra-fraction respiratory motion of the phantom is shown in the first video of Supplementary Material.

The quantification methodology was then performed between all moving sub-cumulative Cherenkov images and the first reference sub-cumulative Cherenkov image in the video, as illustrated in Figure 3F. Non-rigid registration was performed in order to quantify the nonlinear loco-regional deformation during the intra-fraction respiratory motion. A 2D map indicating the local tissue deformation due to the induced respiratory motion was generated for each moving sub-cumulative Cherenkov image. The quantified 2D deformation map for each sub-cumulative Cherenkov image is illustrated in the second video of Supplementary Material. A deformation vector with maximal magnitude was selected as the representative one from each 2D deformation map for testing the rationality of the phantom deformation magnitude and the periodicity of respiratory motion.

2.5 Statistical analysis

All statistical analysis was performed using GraphPad Prism version 10.2.0 for macOS (GraphPad Software, Boston, MA, USA). A paired *t*-test evaluated statistical differences between actual and quantified variations in the phantom study on inter-fraction setup uncertainty. A paired *t*-test was performed to evaluate the statistical differences between the variations

quantified by the rigid registration and non-rigid registration in the retrospective patient study. A P -value of 0.05 or less was considered statistically significant.

3 Results

3.1 Phantom study

The accuracy was validated to be 0.83 ± 0.49 (average \pm 1 standard deviation), ranging from 0.20 to 1.55 mm of discrepancy for the simulated inter-fraction setup uncertainties of couch translations up to 20 mm in three directions illustrated in section 2.4.1. The quantified couch movement was compared to actual couch movement and the accuracy results were plotted in Figure 3D. A paired t -test revealed no significant difference (P value = $0.29 > 0.05$) between actual and quantified couch movement, indicating the accuracy of methodology on quantifying the inter-fraction setup uncertainties. For the test of intra-fractional respiratory motion monitoring, the quantified phantom deformation magnitude in both x and y direction is within the range of 8-10 mm maximum as measured using a physical ruler when the ventilator was on, and the quantified motion varied periodically in agreement with the respiratory pattern.

3.2 Quantifying patient positioning accuracy

With the developed methodology, a retrospective Cherenkov imaging dataset for a cohort of 10 breast cancer patients (including 5 right and 5 left breast cancer patients) was analyzed. The workflow examined the patient setup variations existing among treatment of the 10 patients and the results reveal variation of 3.7 ± 2.4 mm. Some variations are larger than the clinical threshold (3 mm and 3 deg) for several reasons: 1) the translational and rotational discrepancies are

combined in the 2D Cherenkov image domain, leading to larger apparent translational discrepancies; 2) the effect of intra-fractional motion such as respiratory motion is integrated in the cumulative Cherenkov images, contributing to larger discrepancies. Additionally, a 2D deformation map was generated to quantify loco-regional deformation in addition to conventional global shifts, between the first and subsequent fractions. Figure 4A shows the 2D deformation map for each patient between their first and second treatment fraction. Figure 4B shows the comparison of quantified variations from the rigid and non-rigid registration. Net deformation magnitude of 3.3 ± 1.9 mm was quantified as the 95th percentile of all the loco-regional vectors magnitude in the 2D deformation maps generated by the non-rigid registration performed after the rigid registration, demonstrating some loco-regional deformation was remained after the rigid registration and then captured by the non-rigid registration. A mean deformation of 0.12 ± 0.09 mm from all these vectors was quantified, demonstrating the loco-regional deformations are typically in various directions so these pixel-level vectors cancel each other out after adding. Significant differences (paired *t*-test, *P* value < 0.0001) in their quantified variations from two types of registration indicates that the rigid registration captured the majority of global variations, while the non-rigid registration quantifies the residual loco-regional deformations.

4 Discussion

The use of Cherenkov-imaged bio-morphological features in this study marks an advancement in patient positioning techniques for breast radiotherapy. By quantifying loco-regional deformations using segmented bio-morphological features like vasculature, the methodology addresses an aspect of radiation treatment precision that has been previously underexplored. For the first time, local-regional deformation is quantified based on Cherenkov imaged vasculature, opening a new

avenue to improve the precision of patient positioning. The ability to detect and quantify these deformations in real-time has the potential to improve treatment protocols by allowing patient-specific adjustments.

The impact of this methodology extends beyond a technical innovation, representing a step toward personalized radiation therapy treatments. By enabling the precise measurement of tissue deformation during RT, the methodology supports clinicians in making informed decisions regarding dosimetric and position adjustments when necessary as well as rational design of margins to define the PTV. This capability is particularly vital in treatments where millimeter-level precision can significantly influence both the efficacy of tumor targeting and the preservation of surrounding healthy tissues.^{20,21} Furthermore, the bio-morphological features detected through Cherenkov imaging are unique to each individual, which could be applied to verify patient identities through the treatment courses, adding safety redundancy.

Admittedly, there are limitations related to the dimensionality and sensitivity in its current stage. Due to Cherenkov imaging capturing 3D object within 2D imaging space, the current methodology in the phantom study showed heightened sensitivity to variations along vertical and longitudinal directions compared to lateral movements. This sensitivity bias in different dimensions is due to the use of only one camera. A potential solution to overcome this limitation would be using two Cherenkov cameras to reconstruct the 3D patient surfaces with stereovision algorithms, allowing for more accurate spatial quantification of deformations.^{22,23} Other work has demonstrated the feasibility to quantify the setup variations using SGRT system.²⁴ SGRT setup tolerances for breast EBRT are ≤ 3 mm in isocenter position and ≤ 1 degree in gantry

angle.^{25,26(p302)} The 3.7 ± 2.4 mm of global shift and 3.3 ± 1.9 mm of loco-regional deformation quantified indicate the potential value of the methodology in this work to be added on SGRT for more accurate patient setup. This reconstruction results could be potentially integrated to currently deployed SGRT systems, which is work in progress in collaboration with SGRT industrial partners.²⁶ An intrinsic limitation to this technique is that Cherenkov photons are only detected to a depth up to 10 mm meaning that deformations are observed in superficial tissue layers. It is unclear what the relationship is to deeper lying tissues, especially in larger patients.

Additionally, addressing loco-regional deformations remains a complex challenge. The clinical impact of these deformations remains unclear in various scenarios, but the quantification is a crucial step forward for perspective studies evaluating the dosimetric effects. Currently, the segmentation of bio-morphological features is semi-manual, which is not only subjective but also inefficient. A deep-learning approach (e.g., U-Net) is being developed to automate this process, which could significantly enhance the accuracy and speed of vasculature segmentation, enabling segmentation in real-time at the point of image acquisition.^{27,28} Moreover, the applicability of our method is limited to scenarios where bio-morphological features are clearly visible in Cherenkov images. This visibility is often compromised in highly modulated dynamic treatments such as volumetric modulated arc therapy (VMAT), suggesting a need for further technological advancements to adapt this method for broader clinical use.

5 Conclusion

This study introduced a novel application of Cherenkov imaging, utilizing the registration of bio-morphological features to precisely quantify loco-regional tissue deformation. These directly

observed measures from both phantom and human images showed the method's capacity to measure both global and local variations in patient positioning with a high degree of precision. Both rigid and non-rigid registrations of Cherenkov imaged vasculature provide robust methods to quantifying the patient positioning variations and potential inter- and intra-fraction adjustments. Quantified setup variations with level of 3.7 ± 2.4 mm of global shift and 3.3 ± 1.9 mm of loco-regional deformation at 95th percentile of the vector magnitude were observed existing among 10 breast cancer patients but being ignored during their treatment courses. This approach is especially useful for breast cancer radiotherapy given the high amount of soft tissue local deformation that can occur in daily positioning variation. Work is ongoing to integrating this methodology into clinical workflows to provide corrective feedback. This kind of methodology provides one possible path to personalized, precise radiotherapy treatments, optimizing tumor targeting while minimizing exposure to surrounding healthy tissues.

Reference:

1. Siegel RL, Miller KD, Wagle NS, Jemal A. Cancer statistics, 2023. *CA Cancer J Clin.* 2023;73(1):17-48. doi:10.3322/caac.21763
2. Baskar R, Lee KA, Yeo R, Yeoh KW. Cancer and Radiation Therapy: Current Advances and Future Directions. *Int J Med Sci.* 2012;9(3):193-199. doi:10.7150/ijms.3635
3. Jaffray DA. Image-guided radiotherapy: from current concept to future perspectives. *Nat Rev Clin Oncol.* 2012;9(12):688-699. doi:10.1038/nrclinonc.2012.194
4. Bogdanich W. Radiation Offers New Cures, and Ways to Do Harm. *The New York Times.* <https://www.nytimes.com/2010/01/24/health/24radiation.html>. Published January 23, 2010. Accessed November 13, 2023.
5. Jarvis LA, Hachadorian RL, Jermyn M, et al. Initial Clinical Experience of Cherenkov Imaging in External Beam Radiation Therapy Identifies Opportunities to Improve Treatment Delivery. *International Journal of Radiation Oncology*Biological*Physics.* 2021;109(5):1627-1637. doi:10.1016/j.ijrobp.2020.11.013
6. Jarvis LA, Zhang R, Gladstone DJ, et al. Cherenkov Video Imaging Allows for the First Visualization of Radiation Therapy in Real Time. *International Journal of Radiation Oncology*Biological*Physics.* 2014;89(3):615-622. doi:10.1016/j.ijrobp.2014.01.046
7. Newman F, Asadi-Zeydabadi M, Durairaj VD, Ding M, Stuhr K, Kavanagh B. Visual sensations during megavoltage radiotherapy to the orbit attributable to Cherenkov radiation. *Med Phys.* 2008;35(1):77-80. doi:10.1118/1.2815358
8. Steidley KD, Eastman RM, Stabile RJ. Observations of visual sensations produced by Cherenkov radiation from high-energy electrons. *Int J Radiat Oncol Biol Phys.* 1989;17(3):685-690. doi:10.1016/0360-3016(89)90125-9
9. Alexander DA, Decker SM, Jermyn M, et al. One Year of Clinic-Wide Cherenkov Imaging for Discovery of Quality Improvement Opportunities in Radiation Therapy. *Practical Radiation Oncology.* 2023;13(1):71-81. doi:10.1016/j.prro.2022.06.009
10. Andreozzi JM, Zhang R, Glaser AK, Jarvis LA, Pogue BW, Gladstone DJ. Camera selection for real-time in vivo radiation treatment verification systems using Cherenkov imaging. *Med Phys.* 2015;42(2):994-1004. doi:10.1118/1.4906249
11. Decker SM, Alexander DA, Bruza P, et al. Performance comparison of quantitative metrics for analysis of in vivo Cherenkov imaging incident detection during radiotherapy. *BJR.* 2022;95(1137):20211346. doi:10.1259/bjr.20211346
12. Snyder C, Pogue BW, Jermyn M, et al. Algorithm development for intrafraction radiotherapy beam edge verification from Cherenkov imaging. *JMI.* 2018;5(1):015001. doi:10.1117/1.JMI.5.1.015001

13. Brock KK, Mutic S, McNutt TR, Li H, Kessler ML. Use of image registration and fusion algorithms and techniques in radiotherapy: Report of the AAPM Radiation Therapy Committee Task Group No. 132. *Med Phys*. 2017;44(7):e43-e76. doi:10.1002/mp.12256
14. Zhang R, Andreozzi JM, Gladstone DJ, et al. Cherenkov based patient positioning validation and movement tracking during post-lumpectomy whole breast radiation therapy. *Phys Med Biol*. 2014;60(1):L1. doi:10.1088/0031-9155/60/1/L1
15. Decker SM, Alexander DA, Hachadorian RL, et al. Estimation of diffuse Cherenkov optical emission from external beam radiation build-up in tissue. *JBO*. 2021;26(9):098003. doi:10.1117/1.JBO.26.9.098003
16. Detective quantum efficiency of intensified CMOS cameras for Cherenkov imaging in radiotherapy - IOPscience. Accessed April 10, 2024. <https://iopscience.iop.org/article/10.1088/1361-6560/abb0c5>
17. Hachadorian R, Bruza P, Jermyn M, et al. Correcting Cherenkov light attenuation in tissue using spatial frequency domain imaging for quantitative surface dosimetry during whole breast radiation therapy. *JBO*. 2018;24(7):071609. doi:10.1117/1.JBO.24.7.071609
18. B-spline Grid, Image and Point based Registration - File Exchange - MATLAB Central. Accessed April 5, 2024. <https://www.mathworks.com/matlabcentral/fileexchange/20057-b-spline-grid-image-and-point-based-registration?status=SUCCESS>
19. Liu DC, Nocedal J. On the limited memory BFGS method for large scale optimization. *Mathematical Programming*. 1989;45(1):503-528. doi:10.1007/BF01589116
20. Zelefsky MJ, Kollmeier M, Cox B, et al. Improved clinical outcomes with high-dose image guided radiotherapy compared with non-IGRT for the treatment of clinically localized prostate cancer. *Int J Radiat Oncol Biol Phys*. 2012;84(1):125-129. doi:10.1016/j.ijrobp.2011.11.047
21. Dawson LA, Jaffray DA. Advances in Image-Guided Radiation Therapy. *JCO*. 2007;25(8):938-946. doi:10.1200/JCO.2006.09.9515
22. Nam KW, Park J, Kim IY, Kim KG. Application of Stereo-Imaging Technology to Medical Field. *Healthc Inform Res*. 2012;18(3):158-163. doi:10.4258/hir.2012.18.3.158
23. Bert C, Metheany KG, Doppke K, Chen GTY. A phantom evaluation of a stereo-vision surface imaging system for radiotherapy patient setup. *Medical Physics*. 2005;32(9):2753-2762. doi:10.1118/1.1984263
24. Kadman B, Takemura A, Ito T, Okada N, Kojima H, Ueda S. Accuracy of patient setup positioning using surface-guided radiotherapy with deformable registration in cases of surface deformation. *J Appl Clin Med Phys*. 2022;23(3):e13493. doi:10.1002/acm2.13493

25. Das IJ, Cheng CW, Fosmire H, Kase KR, Fitzgerald TJ. Tolerances in setup and dosimetric errors in the radiation treatment of breast cancer. *Int J Radiat Oncol Biol Phys.* 1993;26(5):883-890. doi:10.1016/0360-3016(93)90505-p
26. Al-Hallaq HA, Cerviño L, Gutierrez AN, et al. AAPM task group report 302: Surface-guided radiotherapy. *Medical Physics.* 2022;49(4):e82-e112. doi:10.1002/mp.15532
27. Livne M, Rieger J, Aydin OU, et al. A U-Net Deep Learning Framework for High Performance Vessel Segmentation in Patients With Cerebrovascular Disease. *Front Neurosci.* 2019;13. doi:10.3389/fnins.2019.00097
28. Yin XX, Sun L, Fu Y, Lu R, Zhang Y. U-Net-Based Medical Image Segmentation. *J Healthc Eng.* 2022;2022:4189781. doi:10.1155/2022/4189781

Tables and Figures:

Patient No.	Age	Sex	Site	Prescription Dose	Beam energy
1	63	F	Left breast	266 cGy x 16 fx	6 + 10 MV
2	69	F	Left breast	200 cGy x 25 fx	6 + 10 MV
3	69	F	Left breast	266 cGy x 16 fx	6 + 10 MV
4	51	F	Left breast	266 cGy x 16 fx	6 MV
5	68	F	Left breast	266 cGy x 16 fx	6 + 10 MV
6	58	F	Right breast	266 cGy x 16 fx	6 MV
7	67	F	Right breast	200 cGy x 25 fx	6 MV
8	66	F	Right breast	200 cGy x 25 fx	6 MV
9	70	F	Right breast	266 cGy x 16 fx	6 MV
10	73	F	Right breast	180 cGy x 25 fx	6 + 10 MV

Table 1. Patient demographics and treatment parameters in breast radiotherapy. The following information is provided for each patient: age at treatment, prescription dose, number of fractions imaged, and radiotherapy beam energy.

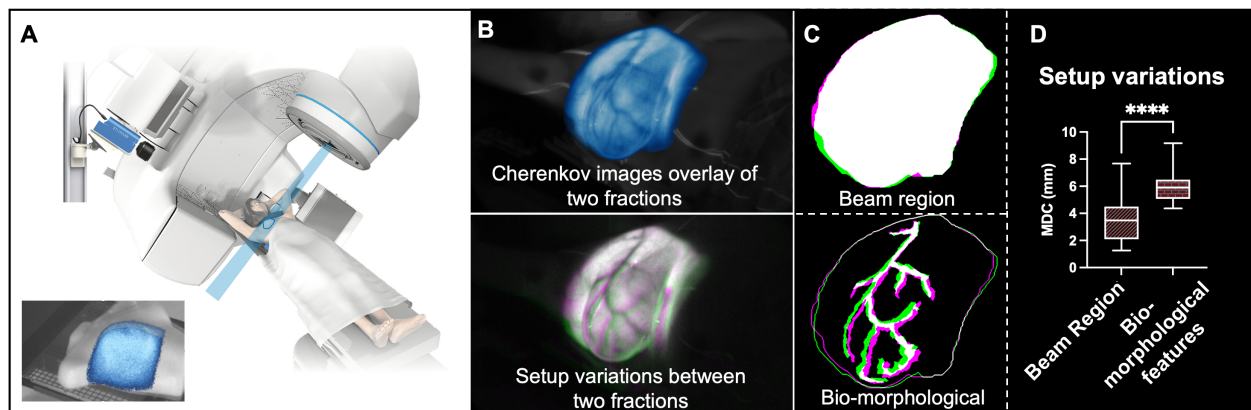


Figure 1. The use of Cherenkov imaging for monitoring patient setup during radiotherapy for breast cancer. (A) Setup of Cherenkov imaging system during treatment. (B) Patient positioning variations captured by the Cherenkov imaging. The top panel shows two Cherenkov images respectively from two fractions of the same patient, each 50% transparently overlaid onto the other to display the positioning variations. Then this two-fraction-overlaid composite image is then superimposed on the background white light image, with a pseudo-colormap applied on Cherenkov images for enhanced visualization. The bottom panel displays the same pair of Cherenkov images but in grayscale and with two different color bands showing their setup variations existing in the two fractions, where the color of magenta represents the variation occurring in the moving image and green represents the reserved part in the reference image. (C) Comparison of observed setup variations between using entire Cherenkov beam region and internal bio-morphological features. (D) Quantified setup variations using the entire Cherenkov beam regions and the internal bio-morphological features respectively, expressed in mean distance to conformity (MDC).

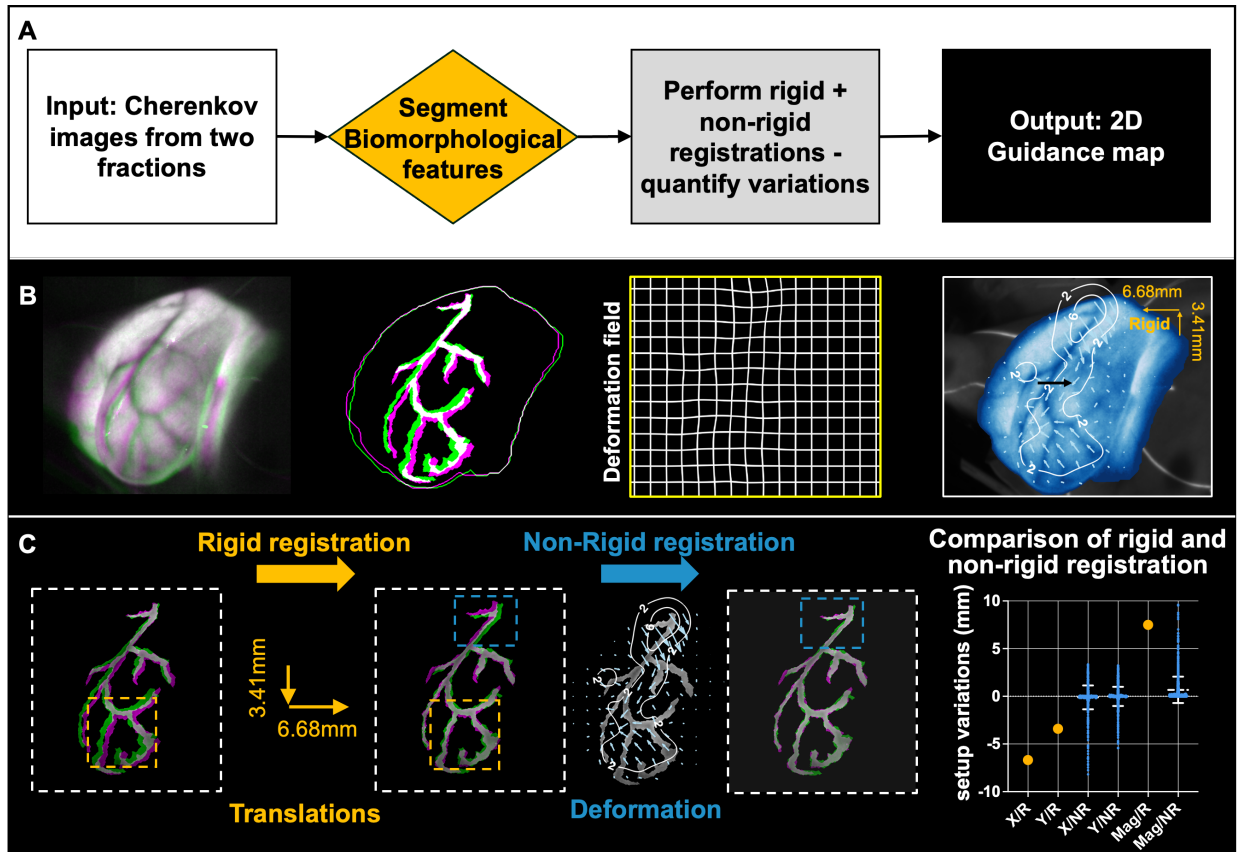


Figure 2. Methodology to quantify patient positioning variations based on bio-morphological features in Cherenkov imaging. (A) Quantification workflow. (B) Example patient Cherenkov image data undergoing this methodology to quantify inter-fraction setup variations. From left to right, each figure represents: Differences between the Cherenkov images of the moving fraction and the reference fraction; Segmentation of bio-morphological features from two fractions and their differences; Deformation field displayed in a grid map quantified from non-rigid registration; Two-dimensional correction guidance map: blue arrows overlaid on the Cherenkov image show the deformation vector for correcting the local deformation from the non-rigid registration, while orange arrows in the upper right corner indicate the global shifts in x and y direction from the rigid registration. The white contour lines are curves along which the magnitude of the deformable correction vectors has a constant magnitude value. (C) Rigid and

non-rigid registration combined workflow illustration. The orange arrows represent the translations from first performed rigid registration and the orange boxes highlight the area where rigid registration improves the alignment of bio-morphological features. The blue map represents the deformation in unit of mm from the non-rigid registration performed sequentially and the blue dotted boxes point out the area where non-rigid registration addresses the remaining loco-regional deformation. The rightmost box plot shows the comparison of variations quantified by the first-performed rigid and sequentially-performed non-rigid registration – in terms of the translation in x, y direction of the imaging plane, and their magnitude. The global variations quantified by the rigid registration were represented by orange points in the box plot, whereas the pixel-level loco-regional deformation quantified by the non-rigid registration were displayed as a distribution displayed in blue, where its mean and one standard deviation shown in white were overlaid on its box plot.

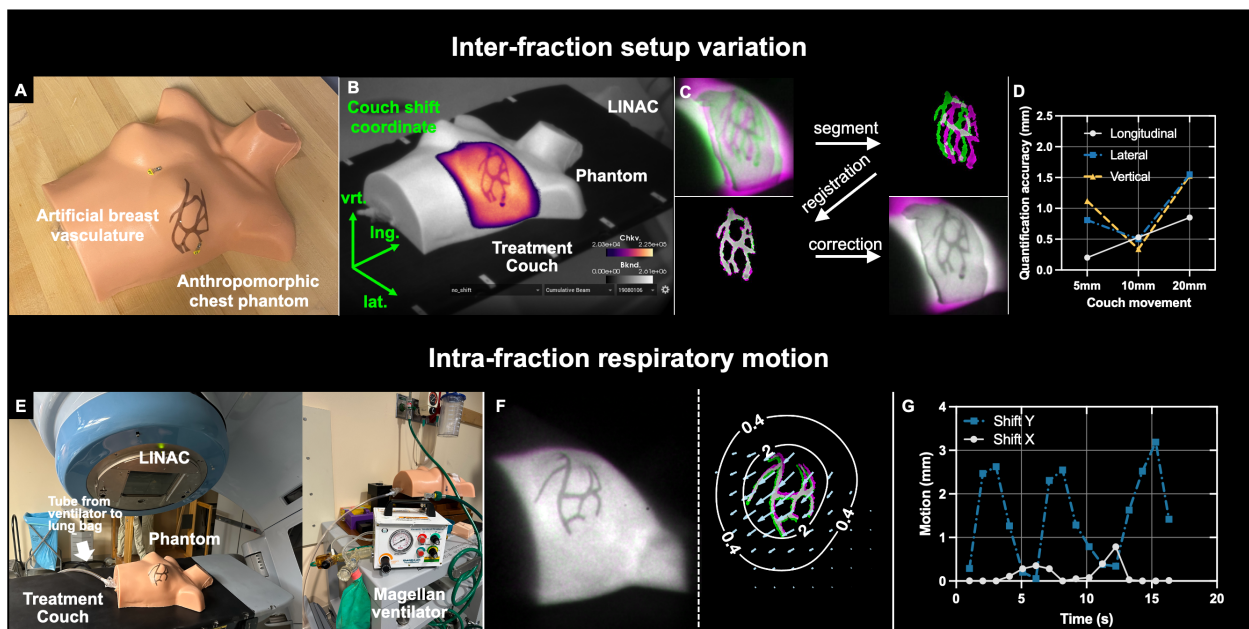


Figure 3. Phantom experiments for testing the methodology quantification accuracy. **(A-D)** Test of quantifying inter-fraction setup uncertainties. **(E-G)** Test of quantifying intra-fraction motions. (A) An anthropomorphic chest phantom with artificial vasculature on the breast surface. (B) Phantom setup with simulated radiotherapy treatment for quantifying inter-fraction setup variations that were simulated by couch movements. (C) Quantification methodology performed on a 20-mm lateral couch movement example. (D) Quantified discrepancies for all couch movements in three directions: lateral, longitudinal, and vertical. (E) Phantom setup for monitoring intra-fraction respiratory motion that were provided by a Magellan ventilator. (F) An example intra-fraction motion quantification result. The left panel shows the differences of Cherenkov images at the inspiration peak and expiration base frames; the right panel shows the deformations quantified by the methodology based on the corresponding bio-morphological features in two frames. The recorded Cherenkov video and the quantified motion video by the methodology based on Cherenkov-imaged bio-morphological features were provided in the Supplementary Material. (G) Quantification results illustrate the quantified respiratory motions in x and y directions of the imaging plane were periodically varying with time.

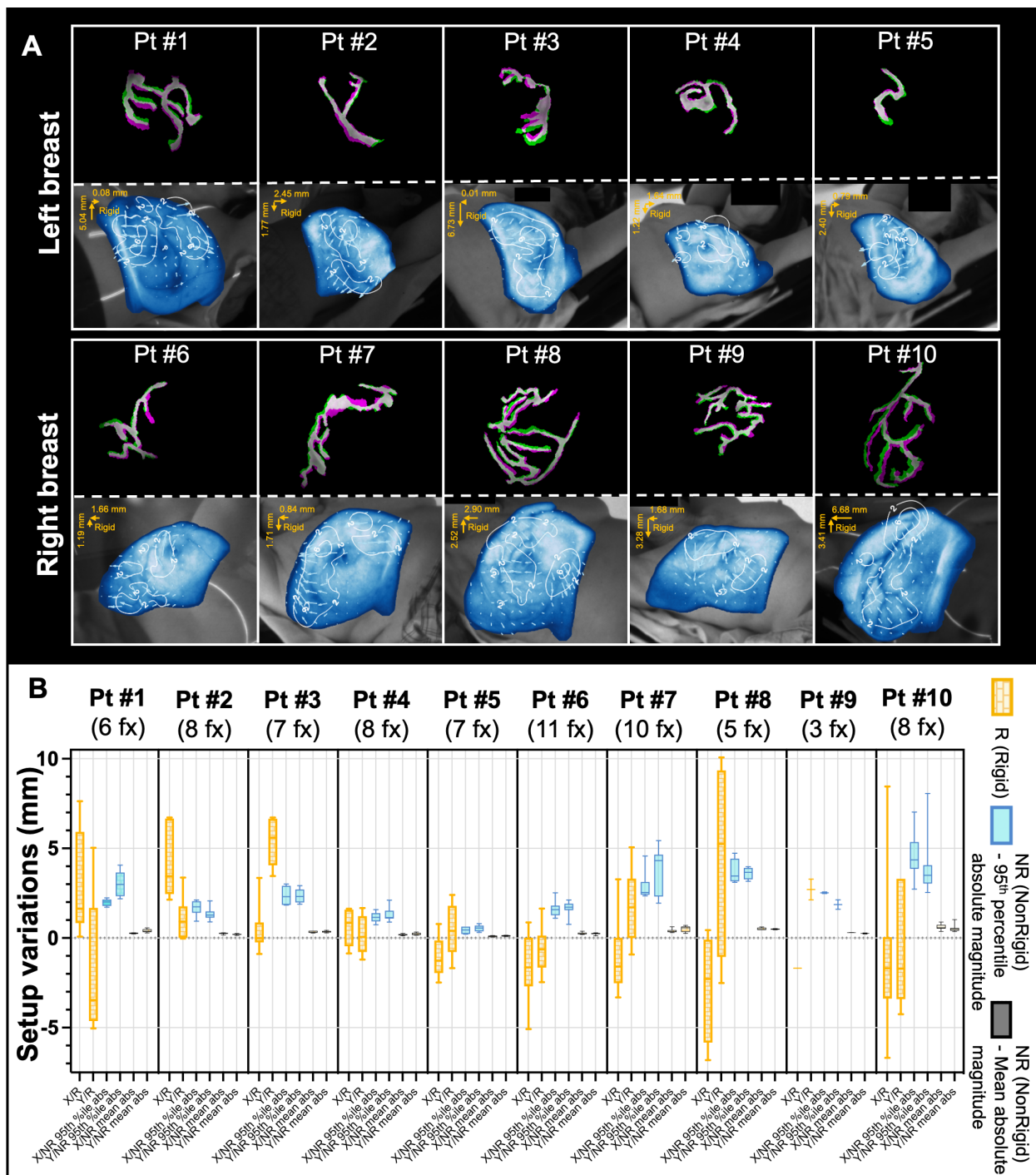


Figure 4. Inter-fraction setup variations quantification results on 10 breast cancer patients (5 left and 5 right). (A) Quantified inter-fraction setup variations existing between their first and second treatment fractions for 10 patients. For each patient, the top panel shows the variations between segmented bio-morphological features of the two fractions. The panel underneath illustrates the

quantified setup variations, including the global shifts (in orange arrows in the upper left corner) from the rigid registration and the loco-regional deformation vectors (in light-blue arrows overlaid on the Cherenkov image) from the non-rigid registration. The white contour are iso-curves with the same deformation magnitude. (B) Comparison of quantified setup variations: the global shifts (orange boxes) from the rigid registration and the loco-regional deformation (blue and black boxes) from the non-rigid registration within all 10 patients in x and y direction of the 2D imaging plane. The blue and black boxes indicate the remaining loco-regional deformations in the quantified 2D map from the non-rigid registration performed after the rigid registration, where blue boxes are the 95th percentile absolute magnitude of vectors in the 2D deformation maps while black boxes are the mean absolute magnitude of these vectors.

Supplementary Material:

Video 1: Cherenkov video for monitoring intra-fraction respiratory motion on phantom.

Video 2: Quantified intra-fraction respiratory motion by the methodology overlaid on the Cherenkov video.